Stony Brook University

Identification and Validation of References Genes for Transcriptome Analysis of Murine Gammaherpesvirus 68 Infection

A Thesis Presented

by

Sandeep Steven-Andrew Reddy

to

The Graduate School

in Partial Fulfillment of the

Requirements

for the Degree of

Master of Science

in

Biochemistry and Cell Biology

Stony Brook University

May 2012

Stony Brook University

The Graduate School

Sandeep Steven-Andrew Reddy

We, the thesis committee for the above candidate for the

Master of Science degree, hereby recommend

acceptance of this thesis.

Dr. Laurie T. Krug, Ph.D., Assistant Professor
Department of Molecular Genetics and Microbiology, Stony Brook University
Thesis Advisor & Principle Investigator

Dr. Nicholas Carpino, Ph.D., Associate Professor
Department of Molecular Genetics and Microbiology, Stony Brook University
Committee Member

This thesis is accepted by the Graduate School

Charles Taber
Interim Dean of the Graduate School

Abstract of the Thesis

Identification and Validation of References Genes for Transcriptome Analysis of Murine Gammaherpesvirus 68 Infection

by

Sandeep Steven-Andrew Reddy

Master of Science

in

Biochemistry and Cell Biology

Stony Brook University

2012

The human gammaherpesviruses (γHV), Kaposi's sarcoma-associated virus (KSHV) and Epstein-Barr virus (EBV), are the etiologic agents of many lymphoproliferative and neoplastic disorders. Murine gammaherpesvirus 68 (MHV68) has a high biological and genetic correlation to EBV and KSHV and represents an amenable, tractable model system to investigate host-virus interactions during chronic γHV infections. Modulating host cellular gene expression is one common strategy utilized during infection by all three viruses. Here, we have shown that four previously reported housekeeping genes (HKGs), *ActB*, *β2M*, *GAPDH* and *HPRT*, evade host shutoff and exhibit stable transcript expression. The validation of these genes in the context of MHV68 infection allowed us to normalize the transcriptional expression of viral *ORF50*, an immediate early gene, by RT-qPCR. The validation of these four genes will allow us to identify additional HKGs with similar attributes that escape virally induced host shutoff. The compilation of these

validated and novel HKGs can then be applied as reference genes to define the transcriptome of gammaherpesvirus infections in multiple cell lines and phases of the viral lifecycle.

DEDICATION

“The universe is change; our life is what our thoughts make it.”

Marcus Aurelius, *Meditations*

To my parents and my siblings,

For supporting my sense of wonder and challenging me to think critically.

TABLE OF CONTENTS

FIGURES

TABLES

ABBREVIATIONS

ActB	β-Actin
β2M	β-2-Microglobulin
bp	base pair *or* base pairs (*contextual*)
$\Delta\Delta C_t$	delta delta (of the) cycle threshold *or* comparative C_t method
CV	coefficient of variation (expressed as a percentage)
cDNA	complementary DNA
C_t	cycle threshold
deJ	de Jonge filtering and ranking method
F	Frerick filtering and ranking method
EBV	Epstein-Barr virus
EBV-CTLs	EBV specific cytoxic T cell lymphocytes, donor-derived
γHV	gammaherpesvirus or gammaherpesviruses (*contextual*)
GAPDH	Glyceraldehydes-6-Phosphate Dehydrogenase
HKG	housekeeping gene
hpi	hours post infection
HPRT	Hypoxanthine-guanine Phosphoribosyltransferase
KS	Kaposi's sarcoma
KSHV	Kaposi's sarcoma-associated herpesvirus
MFC	maximum fold change
MHV68	murine gammaherpesvirus 68
NTC	non-template water control
PCR	polymerase chain reaction

PEL	primary effusion lymphomas
PTLD	post-transplant lymphoproliferative disorders
ORF50	open reading frame 50, murine gammaherpesvirus 68's
RT	reverse transcriptase *or* reverse transcribed (*contextual*)
+RT	reverse transcriptase positive
-RT	reverse transcriptase negative
RTA	replication and transcriptional activator, viral (*see also: ORF50*)
RT-qPCR	quantitative reverse transcribed polymerase chain reaction
SD	standard deviation
SOX	shutoff exonuclease
3S	sort and rank by three criteria

1. Introduction

Gammaherpesviruses exhibit two distinct life cycles.

Gammaherpesviruses (γHV) are double stranded DNA, enveloped viruses that exhibit two distinct lifecycles within the host cell: a productive lytic phase and a latent phase. The two viral life cycles are distinguished by their differences in viral gene expression, the viral genome structure inside of the nucleus and the presence or absence of infectious particles. The lytic phase is characterized by a regulated cascade of gene expression, linear DNA replication and the production of infectious particles. In contrast to the lytic phase, the latent virus persists as a circular, non-integrated episome that is tethered to the host genome, drastically repressed gene expression and lack of viral particle production. Host factors and signals influence the establishment and maintenance of a latent profile and the switch to reactivation from latency to re-enter lytic replication.

The two human gammaherpesviruses are the basis of latency-associated lymphoproliferative and neoplastic diseases.

The γHV Epstein-Barr virus (EBV), Kaposi's sarcoma-associated herpesevirus / human herpesvirus 8 (KSHV / HHV8) and murine gammaherpesvirus 68 (MHV68) predominately establish latency in populations of memory B cells. The establishment of latency in B cells by γHV is also influenced by viral manipulation of host cellular

signaling complexes and pathways. The presence of extrinsic viral forces overriding host signals and checkpoints may lead to the formation of lymphomas and neoplasms (21). KSHV is the etiological agent of Kaposi's sarcoma (KS), primary effusion lymphomas (PELs) and is strongly associated with multimeric Cattleman's disease (13). By comparison, EVB is the cause of infectious mononucleosis and is strongly associated with Burkitt's lymphoma, nasopharyngeal carcinomas, as well as Hodgkin's disease (13). Finally, there exists a high degree of association between γHV reactivation amongst immunocompromised individuals and tumorigenic development; HIV+ patients have increase prevalence of KS as well as Non-Hodgkin lymphomas (29). EBV is the underlying agent to post-transplant lymphoproliferative disorders (PTLD) (16). Current treatment options for patients that develop cancers secondary to γHV infection are limited; for example, clinicians often resort to chemotherapy and monoclonoal antibody treatment (7). Furthermore, current studies using adoptive transfer of donor-derived EBV specific cytoxic T cell lymphocytes (EBV-CTLs) shows promise but are hindered by the time and cost required to generate the cell line, as PTLDs may exhibit rapid progression (7). Therefore it would be advantageous to understand the mechanisms that underlying γHV infection, latency and reactivation and the mechanisms that drive both transformation and tumorigenesis.

MHV68 is a model of γHV that is amenable to the study of natural host-virus pathogenesis.

Murine gammaherpesvirus 68 (MHV68 or γHV68 or murid herpesvirus 4) is a natural pathogen of murine rodents that was originally isolated from bank voles (2) and

is both genetically and biologically related to EBV and KSHV (31). MHV68 represents a tractable experimental system that supports an investigation into *de novo* infections for a wide variety of *in vitro* host cells and *in vivo* studies. MHV68 is a means to assay the molecular basis of host-virus interactions and to develop a deeper understanding into the underlying mechanisms of γHV lytic production, maintenance and establishment of latency and reactivation in a natural host (1). Control of viral gene expression plays a key role in chronic infection.

Viral proteins induce host shutoff during infection and reactivation from latency.

In the context of γHV infection, replication involves an ordered cascade of viral gene expression and regulation beginning with the transcription and translation of immediate-early (IE), then early (E) and lastly late (L) genes (8, 18, 19). The viral replication and transcriptional activator (RTA), encoded by MHV68's open reading frame 50 (*ORF50*) is a transcription factor that is functionally conserved across the γHV. EBV encodes the lytic transactivators BRLF1 and BZLF1/ZTA, and KSHV encodes its own *ORF50* RTA product (17). RTA is responsible for initiating lytic replication upon infection (20) as well as switching the cellular profile of infected cells from latent to lytic, thereby initiating reactivation (17, 23, 34).

In the context of γHV lytic infection, global host gene expression is diminished at the level of RNA stability. Shifting the steady-state equilibrium frees host cellular machinery to generate viral transcripts promoting a lytic phenotype and decreasing the anti-viral and cellular stress responses exhibited by the host (9, 10). Cellular gene expression down regulation by γHV is thought to occur through various means that

preferentially target both messenger RNA (mRNA) and RNA polymerase II (RNApolII). Such strategies include transcriptional blockage, interference of mRNA processing events, blockage of mRNA's export from the nucleus to the cytosol, interference in translational events and direct transcript destabilization (9, 10).

The shutoff exonuclease (SOX) of KSHV's *ORF37* is chiefly responsible for mediating host shutoff by manipulating the cytosolic 5' → 3' exonuclease Xrn1 (9, 10). Each γHV encodes a homolog of SOX; MHV68 encodes murine SOX (muSOX) with its *ORF37* and EBV encodes BGLF5 (9, 10).

In uninfected cells, Xrn1 is dependent on the catalytic activity of Dcp1 and Dcp2 to remove mRNA's specialized 5' – 5' cap prior to exercising its exonuclease activity (22). Deadenylation of mRNA's cap and degradation by Xrn1 decreases the overall abundance of the transcript and therefore reduces gene expression. During infection SOX and Xrn1 act in a concerted manner: SOX seeks out and cleaves mature mRNAs in an endonucleolytic manner, exposing newly created 5' and 3' ends; Xrn1 is then able to degrade the mRNA fragment with the exposed 5' end thereby reducing overall gene expression (9, 10). In addition to bypassing traditional mRNA degradation via cellular Xrn1, the presence of SOX in the cytosol signals the cell to relocalize poly(A) binding proteins (PABPCs) back to the nucleus causing hyper-adenylation of host mRNAs, leading to a blockage of export functions in the nucleus (9, 10).

During host shutoff there are transcripts that avoid degradation through currently unknown mechanisms. Recent studies suggest that transcripts that are more abundant appear to be degraded more efficiently (9, 10). This suggests that although there are widespread changes in host gene expression in the context of viral infection, host

cellular transcripts whose abundance is neither too great nor too little are able to avoid host shutoff. We hypothesize that determining one or more transcripts whose abundance remains unaltered during host shutoff would allow us to normalize the transcript kinetics displayed by both the virus and the host.

Determination of housekeeping genes yields transcriptional analysis by the $\Delta\Delta C_t$ method.

The determination of a gene or set of genes whose expression remains unaltered or is altered only slightly in the context of infection would allow one to account for the changes in mRNA abundance after γHV infection. There exists genes that are constitutively expressed under a wide variety of conditions and tissues, so called “internal control standards” or “housekeeping genes” (HKGs) (28, 32). However, the expression level of these genes in the context of γHV infection has not been validated. HKGs maintain the basal level of cellular transcript expression in order to maintain normal cellular physiology (6). β-Actin (*ActB*), β-2-Microglobulin (*β2M*), Glyceraldehyde-6-Phosphate Dehydrogenase (*GAPDH*) (28) and Hypoxanthine-guanine Phosphoribosyltransferase (*HPRT* or *HPRT1*) (15) are four previously published and widely accepted HKGs utilized experimentally as internal controls in RT-qPCR and as loading controls for protein-immuno blots.

Quantitative reverse transcribed (RT) polymerase chain reaction (RT-qPCR) is a common tool in molecular biology implemented for the quantification of gene expression. Quantitative RT-PCR relies on the intercalation of a fluorescent signal into the polymerized amplimer product during the exponential growth phase of the PCR

cycle. The cycle threshold (C_t) is the cycle at which the fluorescence incorporation overcomes background signal. The C_t is inversely related to transcript abundance (27). A relative change in gene expression, represented as fold change, is calculated by first subtracting the C_t value of the gene of interest from the C_t value of the housekeeping gene (ΔC_t), followed by a second subtraction of the ΔC_t determined for the mock from the ΔC_t of an experimental time point ($\Delta\Delta C_t$). The final fold change is calculated as such (5, 26, 27):

$$\text{Fold Change} = 2^{-\Delta\Delta Ct}$$

Ideally, identification of one or more HKGs as reference genes with RT-qPCR will better enable us to determine the degree of alteration in cellular transcript abundance to be examined in the context of MHV68 infection.

Murine Gammaherpesvirus 68 displays dynamic transcript kinetics during microarray analysis.

In an effort to determine host transcript stability while investigating the interplay between viral infection and host gene expression, microarray analysis of NIH 3T3 murine fibroblasts *de novo* infected with WT MHV68 during an 18 hour time course was conducted using two custom 8 by 15,000 tiled microarrays and two custom 4 by 44,000 tiled microarrays (8). The results demonstrated the dynamic nature of MHV68 transcription upon infection and that viral ORFs were detectable as early as 4 hours post infection (hpi), such was the case with the previously classified immediate-early (IE) gene *RTA*. These data correlated with previously published reports of MHV68 infection kinetics (12, 24).

Understanding the degree of alteration made to host gene expression in the context of MHV68 infection of murine fibroblasts will yield crucial insight into the pathogenesis of γHV infections. There are indications that some genes remain stable thereby evading virally induced host shutoff, such as *β-Actin* and *GAPDH*. We hypothesize that HKGs would be stable during infections at the transcript level. To test this we utilized microarray and bioinformatic analysis to determine if our HKGs could be implemented as reference genes for future quantitative analysis on genome wide transcriptional studies.

2. Results

Bioinformatic analysis predicts stable host transcripts.

Within the context of γHV infections, the effects of SOX mediated host shutoff results in diminished cellular gene expression (9, 10). Housekeeping genes (HKGs) exhibit a degree of stability over a wide variety of conditions (28, 32) but an investigation into their stability has not been determined in the context of γHV infections. Examining the degree of alteration made to host gene expression in the context of γHV infection is an important aspect of investigating host-virus interactions. We examined host gene expression over an 18 hour time course upon MHV68 *de novo* infection to test the hypothesis that during γHV infections the host cell expresses genes that evade viral shutoff.

Our laboratory had previously performed four microarray experiments using RNA samples from various fibroblast infection conditions. These arrays were designed to analyze both viral and cellular genes. To identify housekeeping genes that would provide a set of genes to use for normalization by the $\Delta\Delta C_t$ method, the arrays were loaded with 813 probes for cellular genes previously reported to be stable in a large database analysis (11, 15). From these microarray data we generated a spreadsheet of 1,233 genes common to all four arrays. We utilized the normalized $\log_2$ green signal and eliminated all genes with a value of 0.0. This resulted in a list of 916 genes represented on all four arrays. We then more closely examined four commonly used

HKGs, β-Actin (*ActB*), β-2-Microglobulin (*β2M*), Glyceraldehyde-6-Phosphate Dehydrogenase (*GAPDH*) and Hypoxanthine-guanine Phosphoribosyltransferase (*HPRT*).

Table 1 summarizes our bioinformatic analysis of these four HKGs. We used three methods to determine the merits of an optimal HKG. We determined the mean, standard deviation (SD), coefficient of variation (CV) and maximum fold change (MFC). The MFC is the difference between the maximum and minimum value of fluorescence generated during microarray analysis. We implemented two previously published criteria, deJ (11) and F (15), filtering and determining their rank amongst the 916 genes. No single housekeeping gene met the criteria of those methods for all arrays. These data are suggestive that the criteria for determining HKGs in the context of γHV infections may not meet the criteria of previously published methods for determining optimal HKGs. Thus, we ranked the genes based on a sort of SD, CV and MFC from small to large (3S). *β2M* and *GAPDH* consistently rank higher than *ActB* and *HPRT*.

The Array 1 microarray data for 52 representative cellular genes at 0, 6, 12 and 18 hpi were subjected to hierarchical clustering using uncentered correlation for the similarity metric calculation and complete linkage as the clustering method. From the heat map in Figure 1, it is evident that the HKGs, *ActB*, *β2M*, *GAPDH* and *HPRT*, exhibit stability at the transcript level. However, it should be noted that since the array design was biased towards putative housekeeping genes there are few examples of extreme changes in gene expression.

Table 1. Bioinformatic Analysis of Putative Reference Genes.

	Gene Symbol	Mean	SD	CV (%)	MFC	Rank		
						3S[a]	deJ[b]	F[c]
Array 1	*ActB*	6.040	0.670	11.089	2.2	901	--	--
	β2M	11.525	0.362	3.144	0.9	14	25	301
	HPRT	13.379	0.677	0.051	2.4	127	--	738
	GAPDH	15.108	0.494	3.269	1.6	19	160	440
Array 2	*ActB*	6.944	2.282	32.855	7.1	811	--	--
	β2M	11.179	1.409	12.601	4.3	77	--	--
	HPRT	13.565	1.742	12.845	5.1	80	--	--
	GAPDH	13.817	1.531	11.078	4.3	43	--	--
Array 3	*ActB*	11.157	0.062	0.552	0.1	20	92	111
	β2M	14.612	0.176	1.205	0.2	45	189	250
	HPRT	16.445	0.610	3.711	0.9	175	499	594
	GAPDH	17.921	0.786	4.385	1.1	239	664	771
Array 4	*ActB*	10.947	3.451	31.523	10.3	890	--	--
	β2M	19.202	1.151	5.995	3.4	254	--	--
	HPRT	22.192	1.144	5.155	3.1	118	--	--
	GAPDH	24.724	0.981	3.966	2.8	17	--	787

Genes are ranked against 916 common genes.

SD, standard deviation; CV, coefficient of variation (expressed as a percentage); MFC, maximum fold change; two hyphens (dash mark), indicates that the gene did not meet the criteria;

[a]3S, sorted and ranked using three criteria sorted in the following order and ranked small to large: SD, CV and MFC;

[b]deJ, filtered using previously published criteria (11) in the following order and sorted small to large using the same fields to determine rank: CV<15% (where 15% represents "small") and MFC<2;

[c]F, filtered using previously published criteria (15) in the following order and sorted small to large using the same fields to determine rank: SD<1 and CV≤10%.

Figure 1. **Microarray Analysis of Host Cellular and Housekeeping Genes**. Gene expression patterns of 52 host genes in NIH 3T3 fibroblasts during an 18 hour *de novo* time course infection with WT MHV68. Arrows indicate putative reference genes examined in this study.

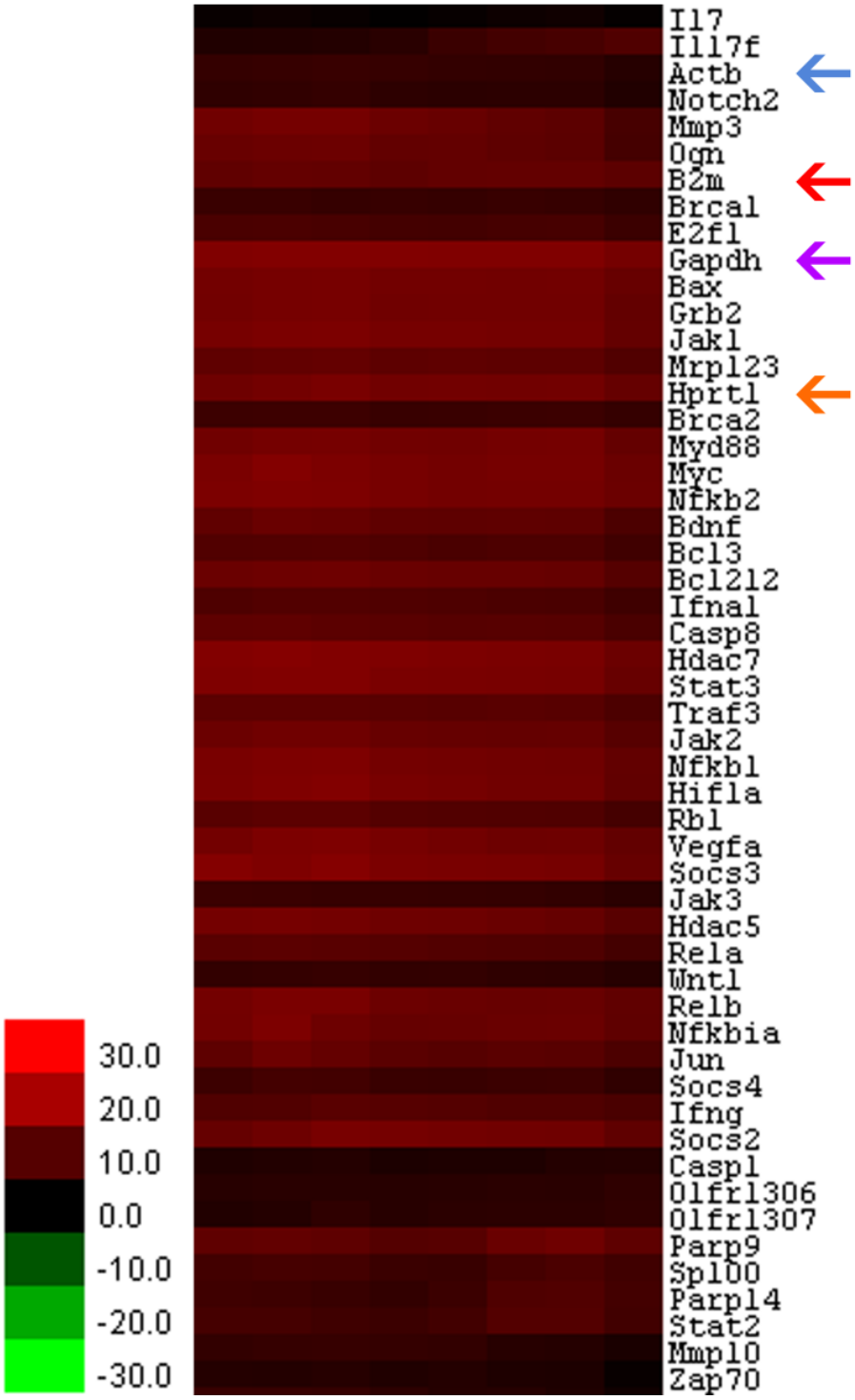
Il7
Il17f
Actb
Notch2
Mmp3
Ogn
B2m
Brca1
E2f1
Gapdh
Bax
Grb2
Jak1
Mrpl23
Hprt1
Brca2
Myd88
Myc
Nfkb2
Bdnf
Bcl3
Bcl2l2
Ifna1
Casp8
Hdac7
Stat3
Traf3
Jak2
Nfkb1
Hif1a
Rbl
Vegfa
Socs3
Jak3
Hdac5
Rela
Wnt1
Relb
Nfkbia
Jun
Socs4
Ifng
Socs2
Casp1
Olfr1306
Olfr1307
Parp9
Sp100
Parp14
Stat2
Mmp10
Zap70
30.0
20.0
10.0
0.0
-10.0
-20.0
-30.0

PCR validates known housekeeping genes.

HKGs are genes whose transcript stability remains unaltered or only slightly changed in response to changes in culture conditions such as viral infection. The stability of HKG transcripts can be utilized to normalize the changes in gene expression of host and viral transcripts when coupled with the quantitative abilities of RT-qPCR. RT-qPCR is a powerful molecular technique, yet the technical details described in publications describing quantification of HKGs varies. Thus, we utilized the protocols and guidelines for the minimum information for publication of quantitative real-time PCR experiments (MIQE) described by Bustin, S.A. et al. (4, 5) to validate RT-qPCR conditions for our HKGs of interest as described in Table 2. This ensures that future investigations are able to reliably and accurately reproduce data and methods as well as establish consistency between independent inquires (4, 5).

Prior to utilizing the obtained primer pairs as reference genes with RT-qPCR, we examined primer specificity. We first determined whether the primers spanned the cDNA intron-exon junction. cDNA is the complementary, reverse transcribed form of mature, spliced mRNA and is a direct correlation to the transcript levels under optimum reverse transcriptase conditions. The results of PCR using a DNA, a cDNA or an NTC template with primers specific for our putative HKG are shown in Figure 2. In Figure 2A, *ActB* primers were able to amplify a specific intron-less region of both a DNA and a cDNA template which resulted in an amplimer product of 214bp. *β2M* had primers that were able to amplify a cDNA template but not a DNA template; a 300bp amplimer was produced (Figure 2B). During amplification, a cDNA template lacking introns is preferentially amplified more rapidly and quickly becomes the major product of the PCR

reaction compared to a DNA template with the intron sequence. Thus, the lack of amplification with DNA indicates primers span the intron-exon junction and only amplify cDNA under the PCR conditions used.

Much like *ActB*, *GAPDH* primers that annealed to an intron-less region of a DNA template (Figure 2C). Lastly, the *HPRT* primers were unable to produce an amplimer product of a DNA template origin, as this template still contained intervening introns which did not afford the reaction enough time to amplify the region between primers. In comparison, cDNA contains only exons and was amplified during PCR to produce a 176bp product (Figure 2D).

RT-qPCR is highly sensitive towards the detection of amplimers and in order to maintain that high degree of sensitivity we implemented a DNase treatment prior to cDNA synthesis. DNase treatment removes any contaminating DNA that may have been carried over during the RNA isolation stage. The degradation of contaminating DNA ensures the elimination of an artificially high source of template; the presence of DNA during quantitative RT-PCR would result in early detection. The removal of a DNA template and the presence of cDNA allows one to be reliably certain that the cycle threshold value (C_t) is solely dependent on cDNA. *GAPDH* previously produced an amplimer using either DNA or cDNA as a template (Figure 2C). In Figure 3, a PCR reaction utilized *GAPDH* primers and a sample that lacked reverse transcriptase (-RT) was unable to generate a product. Both the +RT and –RT samples were DNase treated. From these data we can state with confidence that the removal of contaminating DNA during cDNA generation was successful and that RT-qPCR experiments contain no contaminating sources of template.

Table 2. PCR Conditions for Cellular Genes

Gene Symbol	MGI Sequence Accession ID	Primer Sequence	Oligo Annealing Temperature (˚C)	Amplimer Size (bp)
ActB	MGI:87904	**FOR** 5' – ACC AAC TGG GAC GAT ATG GAG AAG A – 3'	64.6	214
		REV 5' – TAC GAC CAG AGG CAT ACA GGG ACA A – 3'	66.2	
β2M	MGI:88127	**FOR** 5' – GCT ATC CAG AAA ACC CCT CAA – 3'	60.6	300
		REV 5' – CAT GTC TCG ATC CCA GTA GAC GGT – 3'	66.3	
GAPDH	MGI:95640	**FOR** 5' – GCA CCA CCA ACT GCT TAG – 3'	59.9	175
		REV 5' – GAT GCA GGG ATG ATG TTC – 3'	57.6	
HPRT	MGI:96217	**FOR** 5' – GTA ATG ATC AGT CAA CGG GGG AC – 3'	64.6	176
		REV 5' – CAG CAA GCT TGC AAC CTT AAC CA – 3'	62.8	

Figure 2. **Primers Used to Analyze Housekeeping Genes**.
For each primer pair, DNA or cDNA was used as input to determine whether primers spanned introns for the following housekeeping genes:
(A) β-Actin (*ActB*);
(B) β-2-Microglobulin (*β2M*);
(C) Glyceraldehyde-6-Phosphate Dehydrogenase (*GAPDH*);
(D) Hypoxanthine-guanine Phosphoribosyltransferase (*HPRT*);
Arrows indicated expected amplimer product in base pairs (bp). Ladder control sizes were indicated. Box denotes ladder region that was cropped and aligned for easier size determination. NTC, non template water control.

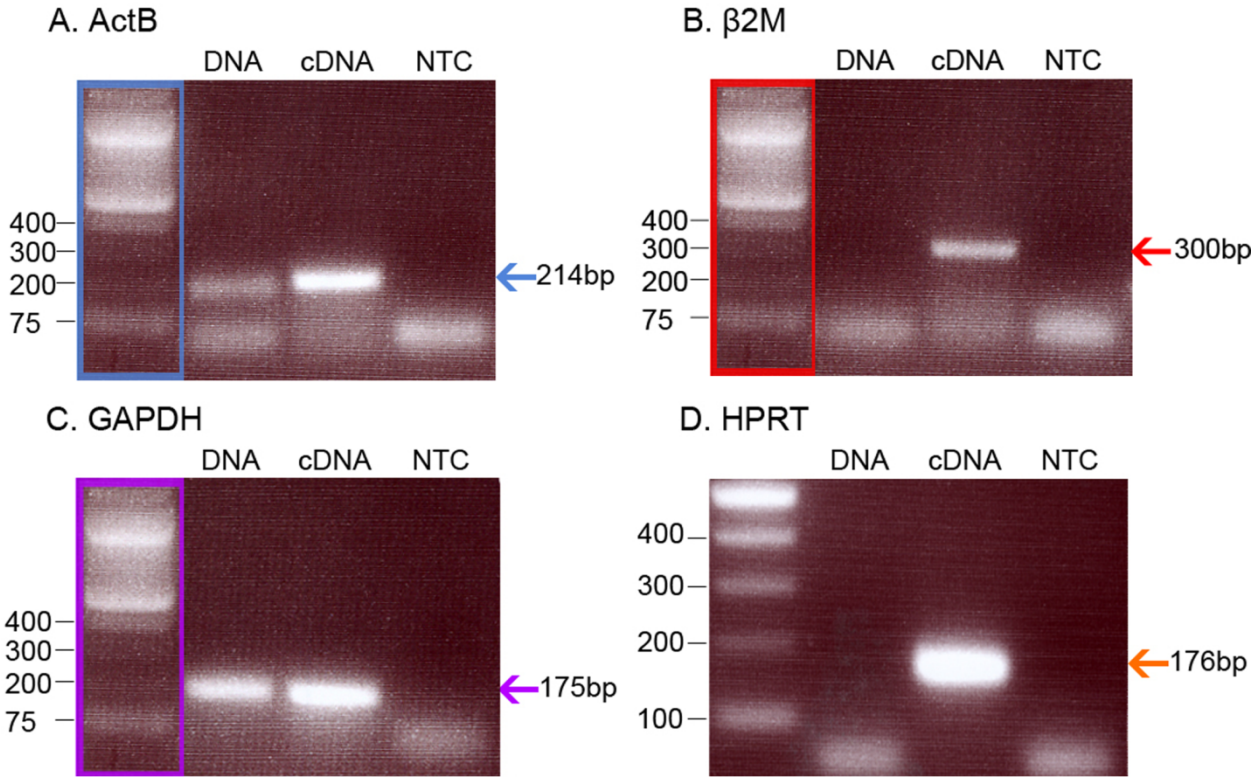
A. ActB
DNA
cDNA
NTC
400
300
200
75
214bp
B. β2M
DNA
cDNA
NTC
400
300
200
75
300bp
C. GAPDH
DNA
cDNA
NTC
400
300
200
75
175bp
D. HPRT
DNA
cDNA
NTC
400
300
200
100
176bp

Figure 3. **Verification of Elimination of Contaminating DNA from RNA Isolation**. DNase treated RNA either reverse transcribed with (+RT) or without (-RT) reverse transcriptase were input into a PCR reaction for *GAPDH*, a housekeeping gene. DNA was the positive input control. Arrow indicated expected amplimer product of 175bp. Ladder control sizes were indicated. NTC, non template water control.

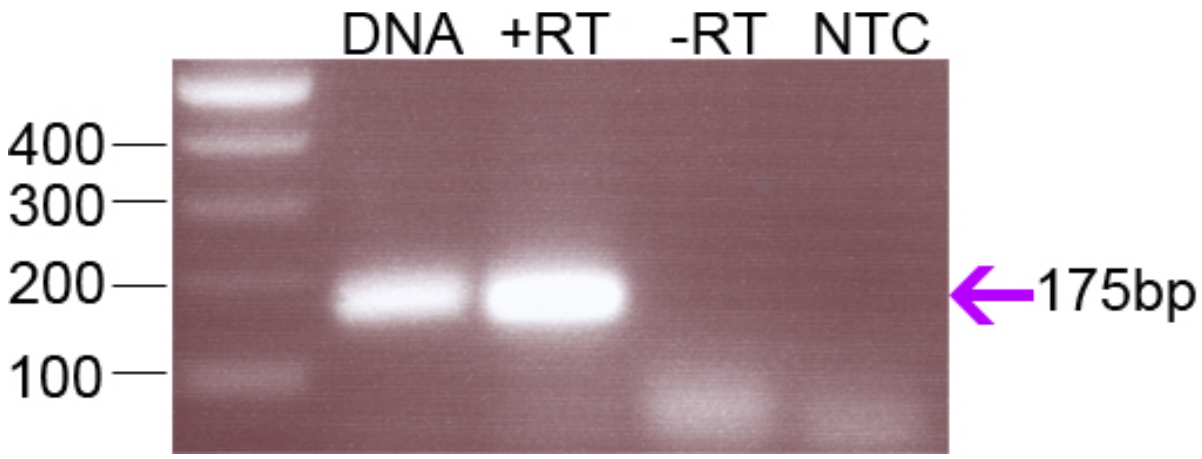
DNA
+RT
-RT
NTC
400
300
200
100
175bp

Housekeeping gene transcripts can be analyzed quantitatively.

In order to quantify the depth of change exhibited by murine fibroblasts in the context of an MHV68 *de novo* infection we utilized RT-qPCR. To determine the lower limits of detection we utilized a PCR reaction whose thermocycler set-up was the same as the RT-qPCR conditons. The PCR reaction utilized a template of cDNA serially diluted in tRNA. tRNA provides constant DNA input and helps prevent primer dimer formation. We then utilized this dilution series, 10^{-1} to 10^{-5}, to generate a standard curve of detection with three to five points (5). The input cDNA was plotted against C_t and subjected to non-linear regression analysis. The PCR efficiency, the efficiency of product doubling with each successive round of PCR, was also determined (5).

The 214bp product of PCR from serial dilutions of cDNA template and primers specific for *ActB* can be detected by PCR with input as dilute as 10^{-5} (Figure 4A). During RT-qPCR, *ActB* generated a 5 log range of detection (Figure 4B). Linear regression generated a slope of -3.356 and the efficiency was 100%. The r^2 value was 0.99297.

Contrasted to *ActB*'s robust display of detection, *β2M*'s lower limit of detection by PCR peaked at 10^{-2} input cDNA in tRNA which produced a 300bp amplimer product (Figure 5A). The sensitivity of RT-qPCR generated a standard curve with a 3 log range of detection (Figure 5B). The resultant slope of the line was -3.450 with an r^2 value of 0.99335. The PCR efficiency was 100%.

PCR with GAPDH primers and a cDNA input diluted down to 10^{-4} produced an amplimer of 175bp (Figure 6A). *GAPDH* primers enabled a 5 log breadth of detection from 10^{-1} to 10^{-5} (Figure 6B). The resultant slope of the line was -3.358 which yielded a PCR efficiency of 100% and an r^2 value of 0.98776.

Lastly, *HPRT*'s lowest limit of detection via PCR was 10^{-1}, which generated the expected 176bp amplimer (Figure 7A). *HPRT* specific primers enabled a 5 log range of detection by RT-qPCR. The resultant slope of the line was -3.332 which yielded a PCR efficiency of 100%. The value of r^2 was .99750.

We conclude that our four putative housekeeping genes exhibited a linear range of detection between three and five points from a template of serially diluted cDNA in a tRNA background. For all four genes, the resultant slope of the line was 100% efficient for PCR amplification and had an r^2 value greater than .98.

Figure 4. **A 5 log Range of Detection with β-Actin (*ActB*) Primers**.
(A) Analysis of amplimer generated from six ten-fold dilutions of input cDNA with primers specific for *ActB*. Arrow indicated expected amplimer product of 214bp. Ladder control sizes were indicated. Box denotes region that was cropped and aligned for easier size determination. NTC, non template water control.
(B) Correlation of cycle threshold (C_t) with input cDNA determined by quantitative RT-PCR. The C_t for SYBR green incorporation was plotted against the input cDNA and analyzed by linear regression analysis by GraphPad Prism version 5.03.

A.

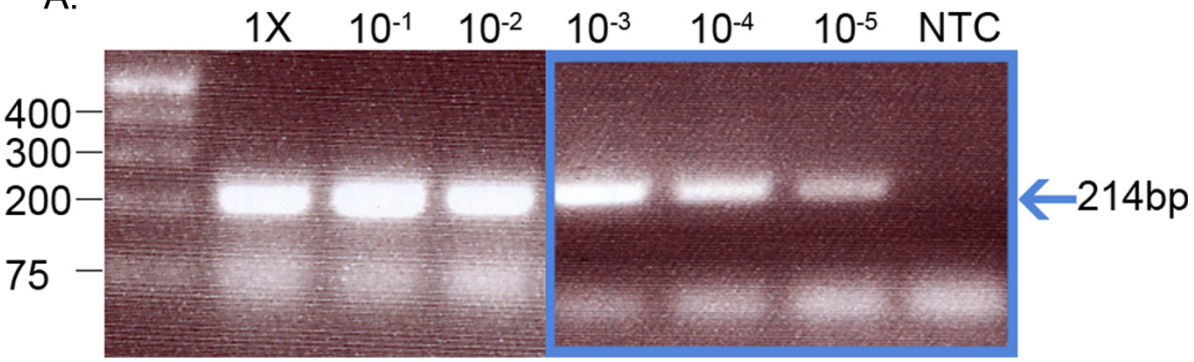
1X
10-1
10-2
10-3
10-4
10-5
NTC
400
300
200
75
214bp

B.

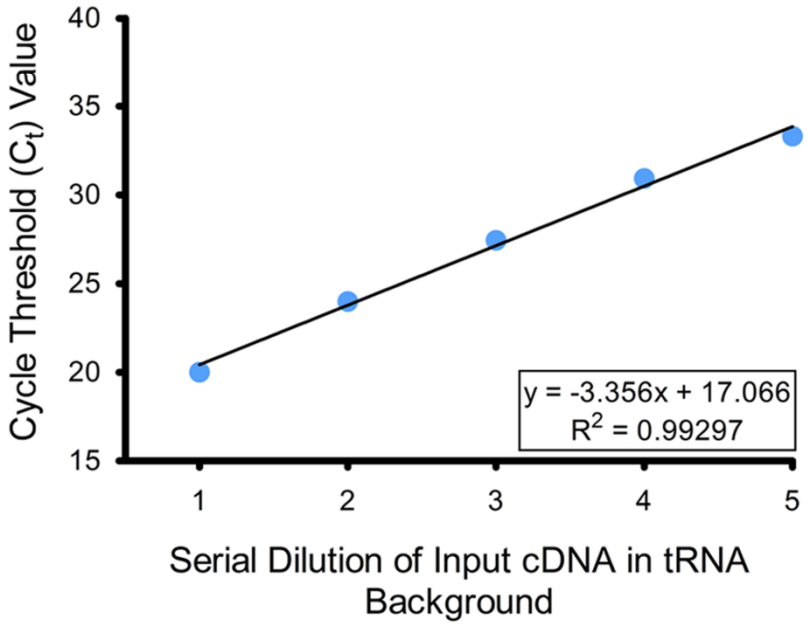
Cycle Threshold (Ct) Value
40
35
30
25
20
15
1
2
3
4
5
y = -3.356x + 17.066
R2 = 0.99297
Serial Dilution of Input cDNA in tRNA Background

Figure 5. **A 3 log Range of Detection with β-2-Microglobulin (*β2M*) Primers**.
(A) Analysis of amplimer generated from six ten-fold dilutions of input cDNA which used primers specific for *β2M*. Arrow indicated expected amplimer product of 300bp. Ladder control sizes were indicated. NTC, non template water control.
(B) Correlation of cycle threshold (C_t) with input cDNA determined by quantitative RT-PCR. The C_t for SYBR green incorporation was plotted against the input cDNA and analyzed by linear regression analysis by GraphPad Prism version 5.03.

A.

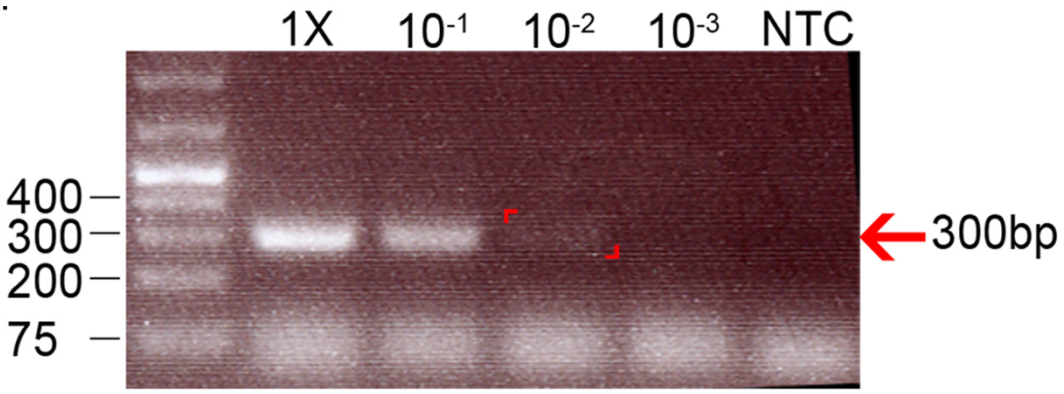
1X
10-1
10-2
10-3
NTC
400
300
200
75
300bp

B.

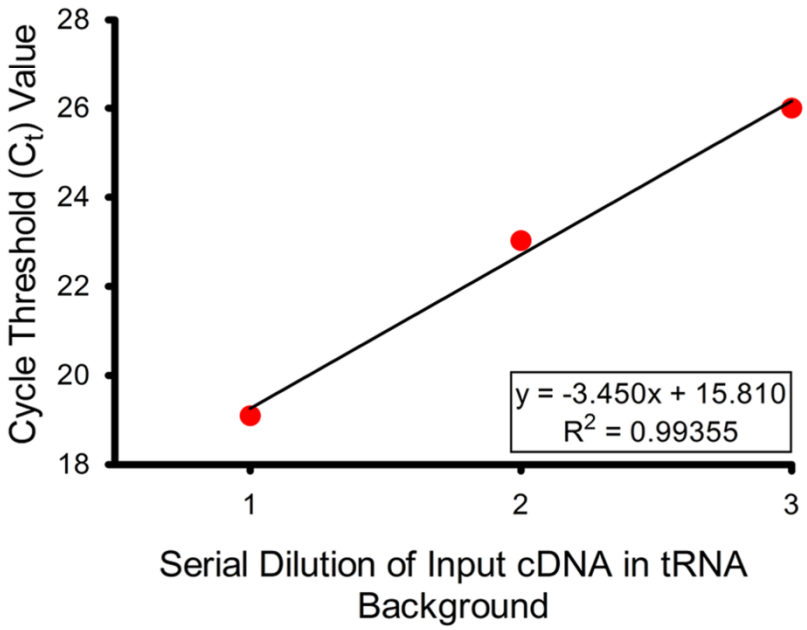
Cycle Threshold (Ct) Value
28
26
24
22
20
18
1
2
3
y = -3.450x + 15.810
R2 = 0.99355
Serial Dilution of Input cDNA in tRNA Background

Figure 6. **A 5 log Range of Detection with Glyceraldehyde-6-Phosphate Dehydrogenase (*GAPDH*) Primers**.

(A) Analysis of amplimer generated from six ten-fold dilutions of input cDNA with primers specific for *GAPDH*. Arrow indicated expected amplimer product of 175bp. Ladder control sizes were indicated. Box denotes region that was cropped and aligned for easier size determination. NTC, non template water control.

(B) Correlation of cycle threshold (C_t) with input cDNA determined by quantitative RT-PCR. The C_t for SYBR green incorporation was plotted against the input cDNA and analyzed by linear regression analysis by GraphPad Prism version 5.03.

A.

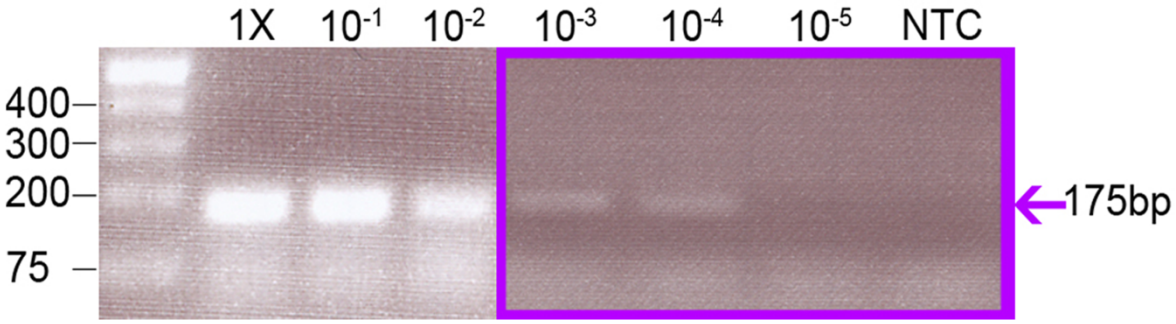
1X
10-1
10-2
10-3
10-4
10-5
NTC
400
300
200
75
175bp

B.

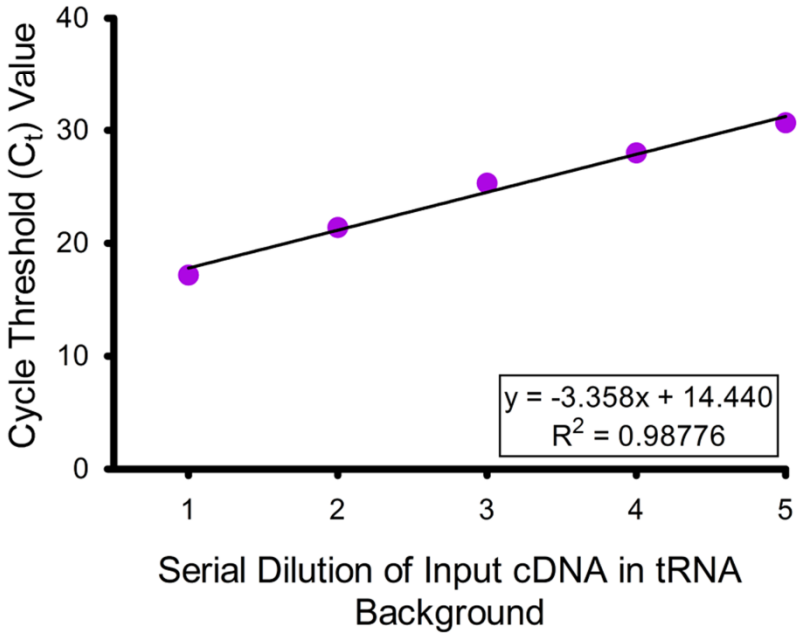
Cycle Threshold (Ct) Value
40
30
20
10
0
1
2
3
4
5
y = -3.358x + 14.440
R2 = 0.98776
Serial Dilution of Input cDNA in tRNA Background

Figure 7. **A 5 log Range of Detection with Hypoxanthine-guanine Phosphoribosyltransferase (*HPRT*) Primers**.

(A) Analysis of amplimer generated from six ten-fold dilutions of input cDNA which used primers specific for *HPRT*. Arrow indicated expected amplimer product of 176bp. Ladder control sizes were indicated. NTC, non template water control.

(B) Correlation of cycle threshold (C_t) with input cDNA determined by quantitative RT-PCR. The C_t for SYBR green incorporation was plotted against the input cDNA and analyzed by linear regression analysis by GraphPad Prism version 5.03.

A.

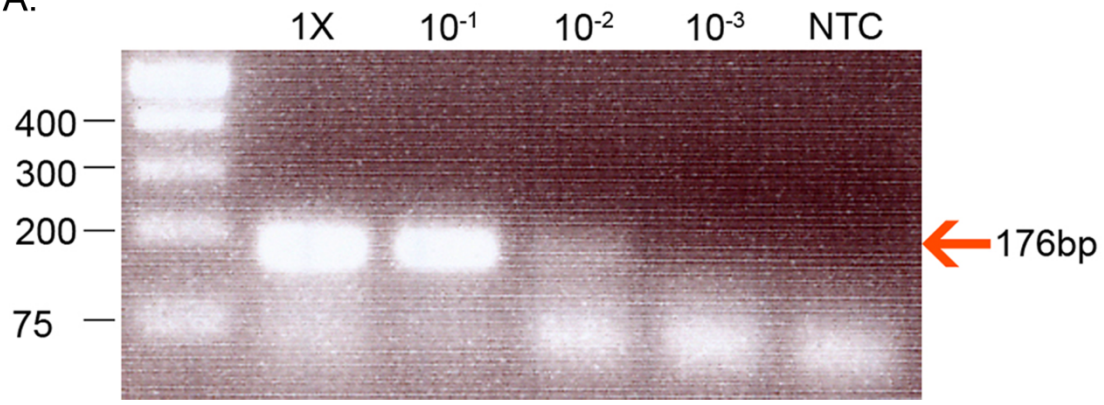
1X
10-1
10-2
10-3
NTC
400
300
200
75
176bp

B.

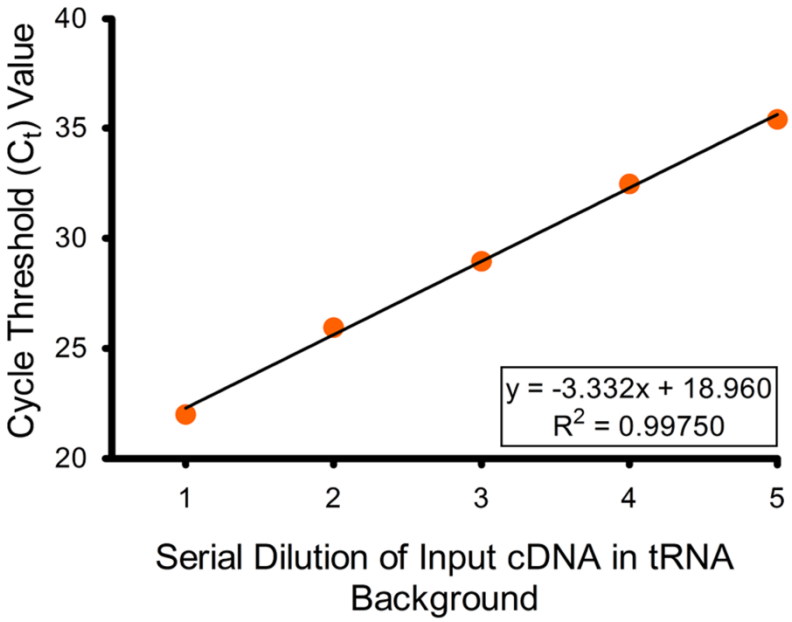
Cycle Threshold (Ct) Value
40
35
30
25
20
1
2
3
4
5
y = -3.332x + 18.960
R2 = 0.99750
Serial Dilution of Input cDNA in tRNA Background

Validation of Putative Reference Genes.

By microarray analysis we established that four cellular transcripts are stable during a *de novo* time course infection of murine fibroblasts. Furthermore, we showed that all four genes exhibited a linear range of detection utilizing RT-qPCR and a cDNA template. We next determined the abundance of each housekeeping gene during the time course of infection to validate their stability and potential use as reference genes to normalize viral and cellular transcripts.

First, we determined the mean C_t value (+/- SD) for each housekeeping gene for one uninfected (0 hpi) and three infected (6, 12, 18 hpi) time points analyzed in triplicate. Relative to each time point within the set, the four housekeeping genes exhibited transcript stability over an 18 hour infection. Relative to one another, *ActB*, *β2M* and *GAPDH* exhibited similar levels of transcript detection (Figure 8A). *HPRT* had slightly greater abundance at each of the 6 hour intervals, as compared to the other three genes at the same points. Based on their stable expression profile during infection, we next utilized these housekeeping genes as reference genes for $\Delta\Delta C_t$ analysis of the viral *ORF50* gene.

Viral *ORF50* transcript expression was normalized to each individual housekeeping gene, which were acting as individual reference genes, at the corresponding time points. The values were then used to determine the fold change relative to the uninfected (0 hpi) time point. Figure 8B displayed the determination of the normalized transcript expression, the resultant $\Delta\Delta C_t$ using a $\log_{10}$ scale. From these data we saw that relative to one another at each time point the fold change of *ORF50* was similar using any of the four reference genes. *ORF50* had a 5 fold change in gene

expression by 6 hpi. By 12 hpi RTA had a 5.5 fold change in transcript expression and a 5.75 fold change in expression at 18 hpi. From these data we conclude that *ORF50* acted as an immediate early gene whose peak activity was approximately 6 hpi as there was very little change in transcriptional expression between 12 and 18 hpi. Next we examined the correlation of *ORF50* transcript levels determined using each reference gene. Irrespective of the housekeeping gene used as the reference gene for the ΔΔCt calculation, the *ORF50* transcriptional profile was similar (Table 3).

Figure 8. **Housekeeping Genes Were Stable and Yielded Similar Normalized *ORF50* Transcript Levels When Used as Reference Genes**.

(A) Housekeeping gene transcripts were stable in the context of an 18 hour *de novo* WT MHV68 infection of NIH 3T3 fibroblasts. Bars represented mean cycle threshold (C_t) value +/- the standard deviation (SD).

(B) Viral *ORF50*'s transcript expression levels determined with the four reference genes were similar. Bars represented the $\Delta\Delta C_t$ value +/- the standard deviation (SD) of *ORF50* normalized to each individual reference gene at 6, 12 and 18 hpi.

A.

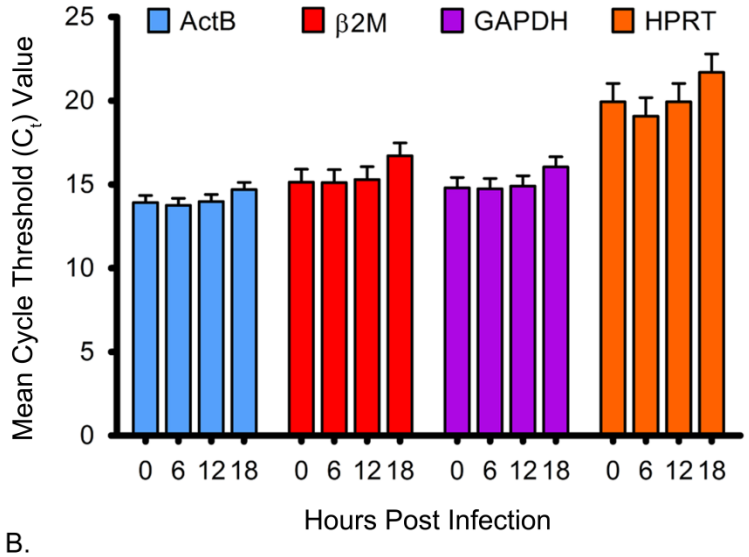
ActB
β2M
GAPDH
HPRT
Mean Cycle Threshold (Ct) Value
25
20
15
10
5
0
0 6 12 18 0 6 12 18 0 6 12 18 0 6 12 18
Hours Post Infection

B.

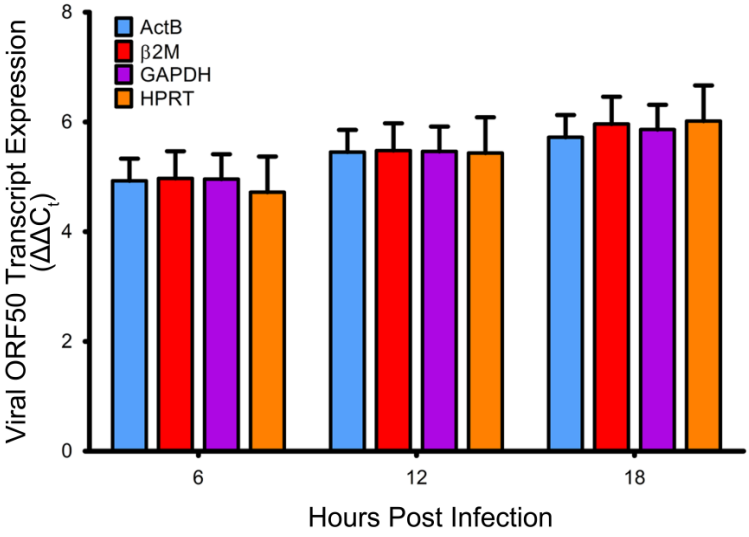
ActB
β2M
GAPDH
HPRT
Viral ORF50 Transcript Expression (ΔΔCt)
8
6
4
2
0
6
12
18
Hours Post Infection

Table 3. **Correlation of *ORF50* Transcript Levels Using Housekeeping Genes**.

	ActB	*β2M*	*GAPDH*	*HPRT*
β2M	0.97607		0.997238	0.99745
GAPDH	0.98951			0.98986
HPRT	0.95974			

Viral *ORF50* transcript levels determined by four housekeeping genes strongly correlated.

3. Discussion

Our laboratory aims to determine changes in host gene expression in the context of viral infections. Host cellular gene expression may be suppressed as a means to promote viral replication. Although a large majority of host genes are diminished at the transcript level there are indications that some genes remain stable, evading host shutoff. We hypothesized that HKGs would be stable during infections at the transcript level. Here we determined that the previously published housekeeping genes (HKGs) β-Actin (*ActB*), β-2-Microglobulin (*β2M*), Glyceraldehyde-6-Phosphate Dehydrogenase (*GAPDH*) and Hypoxanthine-guanine Phosphoribosyltransferase (*HPRT*) had stable transcript levels during an 18 hour *de novo* infection of murine fibroblasts with MHV68. This will enable us to use these HKGs and other similarly behaved genes to be utilized as reference genes for future quantitative analysis on genome wide transcriptional studies.

The four candidate housekeeping genes had stable transcriptional abundance during infection which allowed us to normalize and quantify the rapid increase in the viral *ORF50* transcript levels. The inherent stability possessed by these four genes would suggest that these transcripts evade the phenomena of host shutoff. It would also suggest that, perhaps, other previously published HKGs may too evade host shutoff. The microarray data generated for the four arrays were in the context of another 813 probes for HKGs that were included with the intent of identifying a set of stable genes

for future array designs. The identification of these four stable genes will enable us to utilize the same bioinformatic analysis to validate previously reported and identify additional novel HKGs. Taken together we would then have a suite of genes whose transcriptional expression is stable in the context of γHV infection.

The synergistic cleavage activity of mRNA transcripts by SOX and Xrn1 displayed during KSHV infections suggests sequence specificity rather than positional effects (10). The intrinsic stability possessed by these genes suggests they evade host shutoff. By constructing a gallery of genes we might be able to compare the nucleic acid sequences to identify any features associated with their ability to circumvent host shutoff. In addition to sequence alignments, we will also perform gene ontological studies of the housekeeping genes and other genes that change dramatically. HKGs are stable transcripts in the context of experimental set-ups, thus these studies may yield insight into the types of pathways that the virus preferentially maintains during infection.

Stable transcript levels during infection suggests protein levels would also remain constant. The HKGs *ActB* and *GAPDH* are common loading controls for protein-immuno blots. We expect that *HPRT* and *β2M* will also be useful as loading controls in western blot analysis of gammaherpesvirus infections.

γHV primarily establish latency in memory B cells, yet this study focused on a *de novo* infection of fibroblasts. Research into MHV68 pathogenesis requires the use of multiple cell lines in addition to 3T3 fibroblasts; 3T12 fibroblast lines for *de novo* infections, as well as primary bone-marrow derived macrophages for infections (30), A20 B cells for *de novo* infections and latency establishment investigations and A20-

HE2 MHV68 positive B cells for reaction studies. Thus, the determination of HKGs by similar methods in various cell types and during various points of the viral life cycle will next be investigated and validated prior to utilization as either reference genes in RT-qPCR for comparative C_t experiments or as loading controls for immuno blots.

MHV68 represents a tractable experimental system of γHV that enables the investigation of *de novo* and latent infections, and reactivation from latency in a natural host setting. Previous reports that global host cellular gene expression is diminished in the context of *de novo* MHV68 infection posed a problem to our bioinformatic analysis. Thus, we sought to test whether HKGs maintain a stable level of expression during the coordinated events of virally induced host shutoff. Here we have validated four previously published housekeeping genes, *ActB*, *β2M*, *GAPDH* and *HPRT*, by bioinformatic and RT-qPCR analysis. We then utilized these HKGs as reference genes to normalize the transcriptional profile of the viral immediate early gene *ORF50* in the context of an 18 hour *de novo* infection by the $\Delta\Delta C_t$ method. We will apply the same methods and criteria to validate additional previously published housekeeping genes as well as investigate novel, transcriptionally stable genes. These findings can be applied to additional murine cell lines as well as cell lines at various phases of the MHV68 life cycle to further our understanding of the transcriptional kinetics of γHV pathogenesis.

4. Materials & Methods

Tissue culture of NIH 3T3 and 3T12 fibroblasts.

NIH 3T3 and 3T12 mouse fibroblast cells were maintained in 1X Dulbecco's modified Eagle's medium (DMEM, 1X; Cellgro, Manassas, VA) supplemented with 50 ml of fetal bovine serum (10% FBS; PAA Laboratories, Inc.; Dartmouth, MA), 100 units of penicillin per ml, 100 µg of streptomycin per ml and 2 mM L-glutamine.

Virus preparation and viral infection.

Wild type (WT) murine gammaherpesvirus 68 (MHV68) was passaged and titered as previously described in Weck et al., 1996 (33). NIH 3T3 cells were infected at a multiplicity of infection (MOI) of 10 plaque forming units per ml (PFU/ml) in minimal media for one hour prior to media overlay and time course analysis.

DNA preparation.

Genomic DNA was obtained from NIH 3T12 murine fibroblasts that were mock infected for 12 hours using spin columns from Qiagen's DNeasy Mini Kit according to the manufacturer's recommended protocol (Qiagen; Valencia, CA).

RNA preparation.

RNA was harvested from *de novo* infected NIH 3T3 murine fibroblasts at 0, 6, 12 and 18 hours post infection (hpi) using spin columns from Qiagen's RNeasy Mini Kit according to the manufacturer's recommended protocol (Qiagen; Valencia, CA).

DNase treatment of RNA.

For each time point RNA was DNase treated to remove contaminating DNA using Ambion's TUBRO DNA-free Kit (Invitrogen; Carlsbad, CA). 5 µg of isolated RNA in a 15 µl volume were treated with 1 µl of TURBO DNase and 1.5 µl of 10X TURBO DNase Buffer for 30 minutes at 37˚ C. To this reaction, 1.5 µl of DNase Inactivating Reagent was added and allowed to incubate at room temperature for 5 minutes; this was then centrifuged at 10,000 x g for 90 seconds. The concentration of DNA-free RNA was determined by spectrophotometry of 2 µl using a NanoDrop 2000 Spectrophometer (Thermo Scientific; Pittsburgh, PA); the remaining product was immediately placed into a -80˚ C freezer for long term storage or stored on dry-ice for immediate cDNA synthesis.

cDNA synthesis.

Complimentary DNA (cDNA) was generated through reverse transcription (RT) of 5 µg of DNA-free RNA using Invitrogen's SuperScript III First-Strand Synthesis System for RT-PCR (Invitrogen; Carlsbad, CA). The supplied random hexamers served as the primer template. To ensure the removal of DNA by both Qiagen's RNeasy spin columns

and Ambion's DNase treatment, the negative mock control was treated in the absence of reverse transcriptase (-RT) (Figure 3).

PCR primer designs.

Pertinent information in regards to the putative reference gene PCR primer constructs can be viewed in Table 2. All oligonucleotide designs were obtained from published literature sources: β-Actin (*ActB*), β-2-Microglobulin (*β2M*), Glyceraldehyde-6-Phosphate Dehydrogenase (*GAPDH*) (28), Hypoxanthine-guanine Phosphoribosyltransferase (*HPRT*) (15) and viral open reading frame 50 (*ORF50*) (14). Primers were synthesized by Eurofins MWG/Operon's DNA Sequencing Facility (Eurofins MWG/Operon; Pittsburgh, PA) as a 100 μM stock and were diluted to a 10 μM working solution for both PCR and quantitative RT-PCR.

PCR.

Polymerase chain reaction (PCR) was conducted as a diagnostic to determine whether the putative reference gene primer pair was able to span the exon-intron splice junction. Each reaction consisted of 1X Optimized DyNAzyme Buffer (Finnzymes/Thermo Scientific; Pittsburgh, PA), .2 mM deoxynucleotide solution mix (New England Biolabs; Ipswich, MA), .05 μM of both the forward and reverse primer, .5 U of DyNAzyme II DNA Polymerase (Finnzyme/Thermo Scientific; Pittsburgh, PA). 4 μl of template was added to the aforementioned reaction – wherein template was 3T12-DNA (DNA), mock 12 hour DNA-free RNA reacted with RT (+RT), mock 12 hour DNA-free RNA lacking the reverse transcriptase enzyme (-RT) or PCR grade water (NTC).

Reactions were carried out using an Eppendorf Mastercycler Pro S Thermocycler (Eppendorf; Hauppauge, NY). The program's settings were as follows: 50˚ C for 2 minutes, 95˚ C for 10 minutes, 40 cycles of 95˚ C for 15 seconds followed by one minute of 60˚ C and a final extension of ten minutes at 72˚ C. The products of PCR were visualized on a 1.5% agarose gel (Bioexcell/World Wide Medical Products; Hamilton, NJ).

Quantitative PCR.

Quantitative reverse transcriptase (RT) PCR (quantitative RT-PCR or RT-qPCR) experiments were carried out using an ABI 7300 Real Time PCR System (Applied Biosystems; Foster City, CA). The program settings for both the generation of the standard curve and the $\Delta\Delta C_t$ experiments were as follows: 50˚ C for 2 minutes, 95˚ C for 10 minutes, 40 cycles of 95˚ C for 15 seconds followed by one minute of 60˚ C and a dissociation stage of 95˚ C for 15 seconds, 60˚ C for 30 seconds and 95˚ C for 15 seconds. During the 60˚ C cycling stage, reading of SYBR incorporation into the PCR amplimer occurred.

The standard curve for each putative reference gene (RefGene) was generated using the aforementioned thermocycling program and a 25 µl PCR reaction that consisted of .04 µM of each primer, 1X RT² SYBR Green with ROX qPCR Master Mix (Qiagen; Valencia, CA) and 4 µl cDNA serially diluted in a tRNA background (Sigma Aldrich; St. Louis, MO). The products of RT-qPCR were visualized on a 1.5% agarose gel.

Housekeeping gene and viral *ORF50* transcript expression during an 18 hour *de novo* time course infection was quantified using a similar setup, except for the use of SYBR; in this instance, Qiagen's RT² SYBR Green with ROX qPCR Master Mix was substituted for 1X of PerfeCTa SYBR Green FastMix ROX (Quanta Biosciences, Inc.; Gaithersburg, MD).

The generated data were visualized and initially analyzed using ABI's Sequence Detection Software version 1.2.2 (Applied Biosystems; Foster City, CA).

Statistical analysis.

The data generated by RT-qPCR were further analyzed by Microsoft Excel 2010 (Microsoft Corporation; Redmond, Washington) to generate the mean C_t value for each of the four time points, to determine the standard deviation (SD), to determine the coefficient of variation as a percentage (CV), to determine the maximum fold change (MFC) and to generate both the C_t and $\Delta\Delta C_t$ of each gene (3-5, 26). GraphPad Prism version 5.03 (GraphPad Software, Inc; La Jolla, CA) was used to generate the standard curve for each housekeeping gene as well as to subject the data to a non-linear fit test. Furthermore, the $\Delta\Delta C_t$ expression of viral *ORF50* during the time course of infection was subjected to the same analysis – excluding standard curve generation – along with determination of $\Delta\Delta C_t$ values at each time point normalized to each putative reference gene at the same time point.

Microarray design and bioinformatic analysis.

In an effort to understand the widespread effects of WT MHV68 infection upon NIH 3T3 cells during *de novo* infection, a total of four microarray designs, two 8 by 15,000 and two 4 by 44,000 formats, were made custom by Laurie Krug, Ph.D. in collaboration with Janet Leatherwood, Ph.D., from the Department of Molecular Genetics & Microbiology, and Jizu Zhi, Ph.D., from the Department of Pathology and the Bioinformatics Facility, at Stony Brook University. The designs themselves are detailed in Cheng, B.Y. et al., 2012. All raw data were analyzed and processed by Drs. Krug and Zhi and Mr. Sohail Khan, as described previously (8).

The data generated were subjected to various forms of statistical analysis, described by Table 1. Hierarchical clustering using uncentered correlation for the similarity metric calculation and complete linkage as the clustering method via Cluster version 3.0 (University of Tokyo, Human Genome Center); cluster analysis generated the heat map of a sub-set of Array 1 genes. These genes were visualized by Java TreeView version 1.1.4r3 (Figure 1) (25).

BIBLIOGRAPHY

1. **Barton, E., P. Mandal, and S. H. Speck.** 2011. Pathogenesis and host control of gammaherpesviruses: lessons from the mouse. Annual review of immunology **29:**351-397.

2. **Blaskovic, D., M. Stancekova, J. Svobodova, and J. Mistrikova.** 1980. Isolation of five strains of herpesviruses from two species of free living small rodents. Acta virologica **24:**468.

3. **Bustin, S. A.** 2000. Absolute quantification of mRNA using real-time reverse transcription polymerase chain reaction assays. Journal of molecular endocrinology **25:**169-193.

4. **Bustin, S. A.** 2010. Why the need for qPCR publication guidelines?--The case for MIQE. Methods **50:**217-226.

5. **Bustin, S. A., V. Benes, J. A. Garson, J. Hellemans, J. Huggett, M. Kubista, R. Mueller, T. Nolan, M. W. Pfaffl, G. L. Shipley, J. Vandesompele, and C. T. Wittwer.** 2009. The MIQE guidelines: minimum information for publication of quantitative real-time PCR experiments. Clinical chemistry **55:**611-622.

6. **Butte, A. J., V. J. Dzau, and S. B. Glueck.** 2001. Further defining housekeeping, or "maintenance," genes Focus on "A compendium of gene expression in normal human tissues". Physiological genomics **7:**95-96.

7. **Carbone, A., A. Gloghini, and G. Dotti.** 2008. EBV-associated lymphoproliferative disorders: classification and treatment. The oncologist **13:**577-585.

8. **Cheng, B. Y., J. Zhi, A. Santana, S. Khan, E. Salinas, J. C. Forrest, Y. Zheng, S. Jaggi, J. Leatherwood, and L. T. Krug.** 2012. Tiled Microarray Identification of Novel Viral Transcript Structures and Distinct Transcriptional Profiles during Two Modes of Productive Murine Gammaherpesvirus 68 Infection. Journal of virology **86:**4340-4357.

9. **Clyde, K., and B. A. Glaunsinger.** 2011. Deep sequencing reveals direct targets of gammaherpesvirus-induced mRNA decay and suggests that multiple mechanisms govern cellular transcript escape. PloS one **6:**e19655.

10. **Covarrubias, S., M. M. Gaglia, G. R. Kumar, W. Wong, A. O. Jackson, and B. A. Glaunsinger.** 2011. Coordinated destruction of cellular messages in translation complexes by the gammaherpesvirus host shutoff factor and the mammalian exonuclease Xrn1. PLoS pathogens **7:**e1002339.

11. **de Jonge, H. J., R. S. Fehrmann, E. S. de Bont, R. M. Hofstra, F. Gerbens, W. A. Kamps, E. G. de Vries, A. G. van der Zee, G. J. te Meerman, and A. ter Elst.** 2007. Evidence based selection of housekeeping genes. PloS one **2:**e898.

12. **Ebrahimi, B., B. M. Dutia, K. L. Roberts, J. J. Garcia-Ramirez, P. Dickinson, J. P. Stewart, P. Ghazal, D. J. Roy, and A. A. Nash.** 2003. Transcriptome profile of murine gammaherpesvirus-68 lytic infection. The Journal of general virology **84:**99-109.

13. **Elgui de Oliveira, D.** 2007. DNA viruses in human cancer: an integrated overview on fundamental mechanisms of viral carcinogenesis. Cancer letters **247:**182-196.

14. **Forrest, J. C., C. R. Paden, R. D. Allen, 3rd, J. Collins, and S. H. Speck.** 2007. ORF73-null murine gammaherpesvirus 68 reveals roles for mLANA and p53 in virus replication. Journal of virology **81:**11957-11971.

15. **Frericks, M., and C. Esser.** 2008. A toolbox of novel murine house-keeping genes identified by meta-analysis of large scale gene expression profiles. Biochimica et biophysica acta **1779:**830-837.

16. **Gupta, S., F. J. Fricker, R. P. Gonzalez-Peralta, W. B. Slayton, P. M. Schuler, and V. R. Dharnidharka.** 2010. Post-transplant lymphoproliferative disorder in children: recent outcomes and response to dual rituximab/low-dose chemotherapy combination. Pediatric transplantation **14:**896-902.

17. **Hair, J. R., P. A. Lyons, K. G. Smith, and S. Efstathiou.** 2007. Control of Rta expression critically determines transcription of viral and cellular genes following gammaherpesvirus infection. The Journal of general virology **88:**1689-1697.

18. **Honess, R. W., and B. Roizman.** 1974. Regulation of herpesvirus macromolecular synthesis. I. Cascade regulation of the synthesis of three groups of viral proteins. Journal of virology **14:**8-19.

19. **Johnson, L. S., E. K. Willert, and H. W. Virgin.** 2010. Redefining the genetics of murine gammaherpesvirus 68 via transcriptome-based annotation. Cell host & microbe **7:**516-526.

20. **Lukac, D. M., J. R. Kirshner, and D. Ganem.** 1999. Transcriptional activation by the product of open reading frame 50 of Kaposi's sarcoma-associated herpesvirus is required for lytic viral reactivation in B cells. Journal of virology **73:**9348-9361.

21. **Mandal, P., B. E. Krueger, D. Oldenburg, K. A. Andry, R. S. Beard, D. W. White, and E. S. Barton.** 2011. A gammaherpesvirus cooperates with interferon-alpha/beta-induced IRF2 to halt viral replication, control reactivation, and minimize host lethality. PLoS pathogens **7:**e1002371.

22. **Parker, R., and U. Sheth.** 2007. P bodies and the control of mRNA translation and degradation. Molecular cell **25:**635-646.

23. **Pavlova, I. V., H. W. t. Virgin, and S. H. Speck.** 2003. Disruption of gammaherpesvirus 68 gene 50 demonstrates that Rta is essential for virus replication. Journal of virology **77:**5731-5739.

24. **Rochford, R., M. L. Lutzke, R. S. Alfinito, A. Clavo, and R. D. Cardin.** 2001. Kinetics of murine gammaherpesvirus 68 gene expression following infection of murine cells in culture and in mice. Journal of virology **75:**4955-4963.

25. **Saldanha, A. J.** 2004. Java Treeview--extensible visualization of microarray data. Bioinformatics **20:**3246-3248.

26. **Schefe, J. H., K. E. Lehmann, I. R. Buschmann, T. Unger, and H. Funke-Kaiser.** 2006. Quantitative real-time RT-PCR data analysis: current concepts and the novel "gene expression's CT difference" formula. J Mol Med (Berl) **84:**901-910.

27. **Schmittgen, T. D., and K. J. Livak.** 2008. Analyzing real-time PCR data by the comparative C(T) method. Nature protocols **3:**1101-1108.

28. **Schmittgen, T. D., and B. A. Zakrajsek.** 2000. Effect of experimental treatment on housekeeping gene expression: validation by real-time, quantitative RT-PCR. Journal of biochemical and biophysical methods **46:**69-81.

29. **Simard, E. P., and E. A. Engels.** 2010. Cancer as a cause of death among people with AIDS in the United States. Clinical infectious diseases : an official publication of the Infectious Diseases Society of America **51:**957-962.

30. **Tarakanova, V. L., V. Leung-Pineda, S. Hwang, C. W. Yang, K. Matatall, M. Basson, R. Sun, H. Piwnica-Worms, B. P. Sleckman, and H. W. t. Virgin.** 2007. Gamma-herpesvirus kinase actively initiates a DNA damage response by inducing phosphorylation of H2AX to foster viral replication. Cell host & microbe **1:**275-286.

31. **Virgin, H. W. t., P. Latreille, P. Wamsley, K. Hallsworth, K. E. Weck, A. J. Dal Canto, and S. H. Speck.** 1997. Complete sequence and genomic analysis of murine gammaherpesvirus 68. Journal of virology **71:**5894-5904.

32. **Warrington, J. A., A. Nair, M. Mahadevappa, and M. Tsyganskaya.** 2000. Comparison of human adult and fetal expression and identification of 535 housekeeping/maintenance genes. Physiological genomics **2:**143-147.

33. **Weck, K. E., M. L. Barkon, L. I. Yoo, S. H. Speck, and H. I. Virgin.** 1996. Mature B cells are required for acute splenic infection, but not for establishment of latency, by murine gammaherpesvirus 68. Journal of virology **70:**6775-6780.

34. **Wu, T. T., E. J. Usherwood, J. P. Stewart, A. A. Nash, and R. Sun.** 2000. Rta of murine gammaherpesvirus 68 reactivates the complete lytic cycle from latency. Journal of virology **74:**3659-3667.